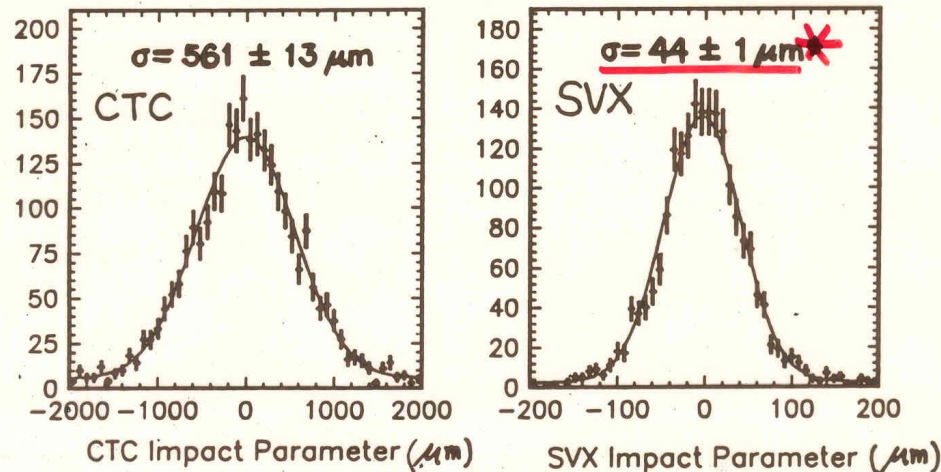


A $10,7 \mu$ residual corresponds to a resolution of $\sim 13 \mu$ on each sensor.



The impact parameter resolution was $\sim 560\mu$ without, and $\sim 44\mu$ with the SVX. Moreover this 44μ resolution was dominated by the beam spot size, which was $\sim 35 \mu$.

MUONS IN CDF

A muon candidate is a CTC track pointing at a segment in the outer chambers.

To discriminate against non-interacting or decaying hadrons

- a) request m.i.p. ionization in the e.m. and in the had. calorimeter
- b) no energy and no momentum flow around the candidate muon track
- c) extrapolate outwards the CTC track and find a good match with a segment in the muon chambers

To discriminate against cosmic muons

- a) request a small track impact parameter relative to primary vertex
- b) Request a small longitudinal distance of track from primary vertex

ELECTRONS IN CDF

A candidate electron is a CTC track pointing at a e.m. cluster in the calorimeter.

To discriminate against photon conversions

- a) request an inner match to the CTC track in SVX and in VTPC
- b) reject tracks coming in pairs of small mass

c) To discriminate against hadrons

- d) request small had/em energy ratio in calorimeter
- e) calorimeter energy should check with CTC momentum
- f) correct profile in shower chamber and small width in e.m. cal.
- g) position in shower chamber should match extrapolated CTC track
- h) request no energy and no momentum flow around track

Overall efficiency of hadron discrimination depends on how tight or loose cuts are made. Typically $\epsilon \sim 80\%$.

JETS IN CDF

An energy cluster is built by adding the energy of adjacent towers which are above 2 GeV.

The integration is extended to a circle in the η , ϕ space, whose radius $R = \sqrt{(\eta^2 + \phi^2)}$ depends on the process being studied. For 2 jet events, $R = 1.0$. For multi-jet events like in the top search, $R = 0,4$.

The corrections to be applied to derive the full jet energy depend on R and are computed with Monte Carlo simulation which uses in input the measured energy density far from the jet axis.

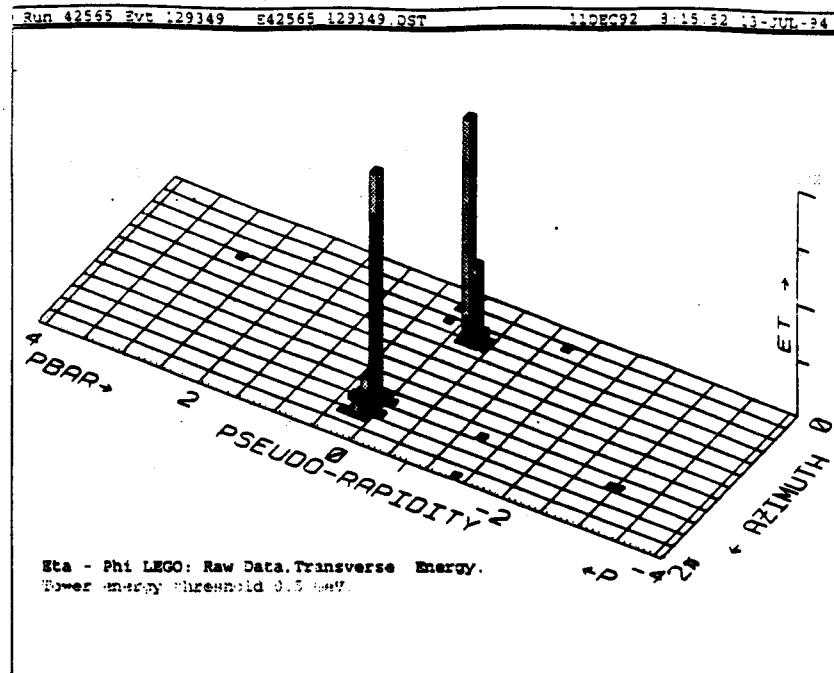
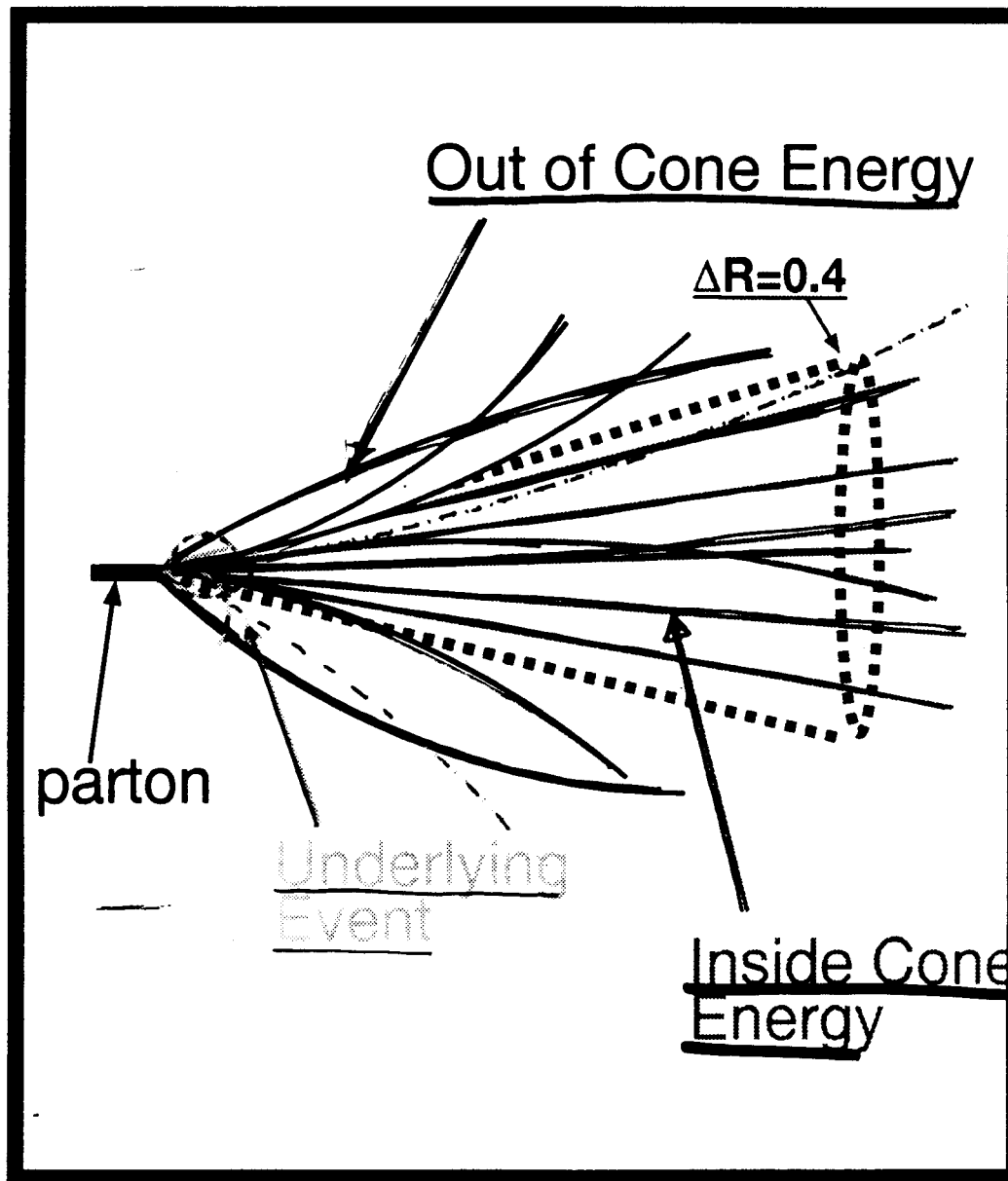


Figure 4: Lego plot for a spectacular two-jet event observed in the CDF detector.

CORRECTIONS TO THE RAW JET ENERGY

The jet energy in a η, φ cone of radius R must be corrected for

- a) Energy lost outside the cone. This correction depends on R , on the jet energy and on the theoretical cross section to which the results are going to be compared. For $R = 0,7$ and for $E_j > 100$ GeV, if the cross section is computed to NLO this correction is negligible;
- b) Energy integrated inside the cone but contributed by the soft underlying interaction of partons not participating in the hard collision. This correction can be estimated by measuring the E_t density far from the jet cones. For $R = 0.7$ it is of about 1 GeV, with negligible dependence on jet energy.



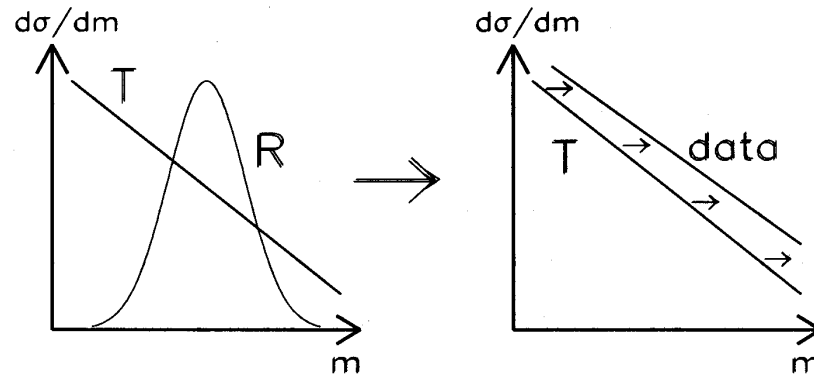


Figure 4.3: The finite detector resolution leads to a *smearing* of the true differential cross section. The observed distribution (the data) is shifted with respect to the true distribution.

When the steep cross section is measured with finite jet energy resolution, in average jets appear to possess higher energies. CDF compares the experimental cross section to the theoretical one smeared for this resolution effect.

In order to compute the jet cross section starting from theory of parton scattering one must know how partons fragment into observable hadron jets.

This is a non perturbative process. It can still to some extent be controlled by performing higher order calculations, whereby more than 2 partons are produced in the hard collision. However, hard partons originating jets can be produced in the fragmentation process as well. These effects are simulated by Monte Carlo programs. In some of these programs perturbative cross sections are still used to compute gluon radiation during the initial fragmentation process, as long as the momentum transfer is considered large enough.

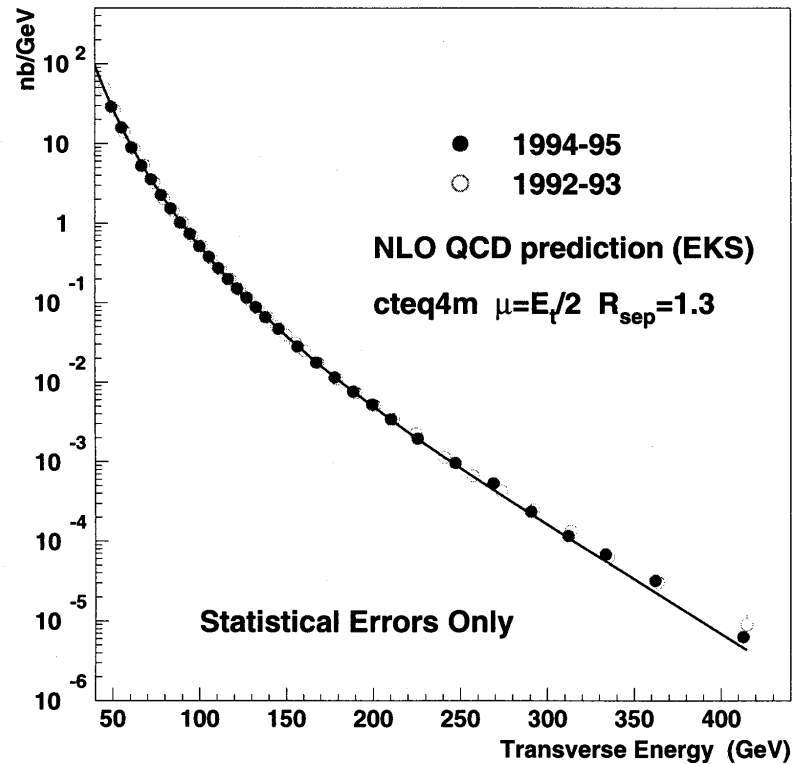
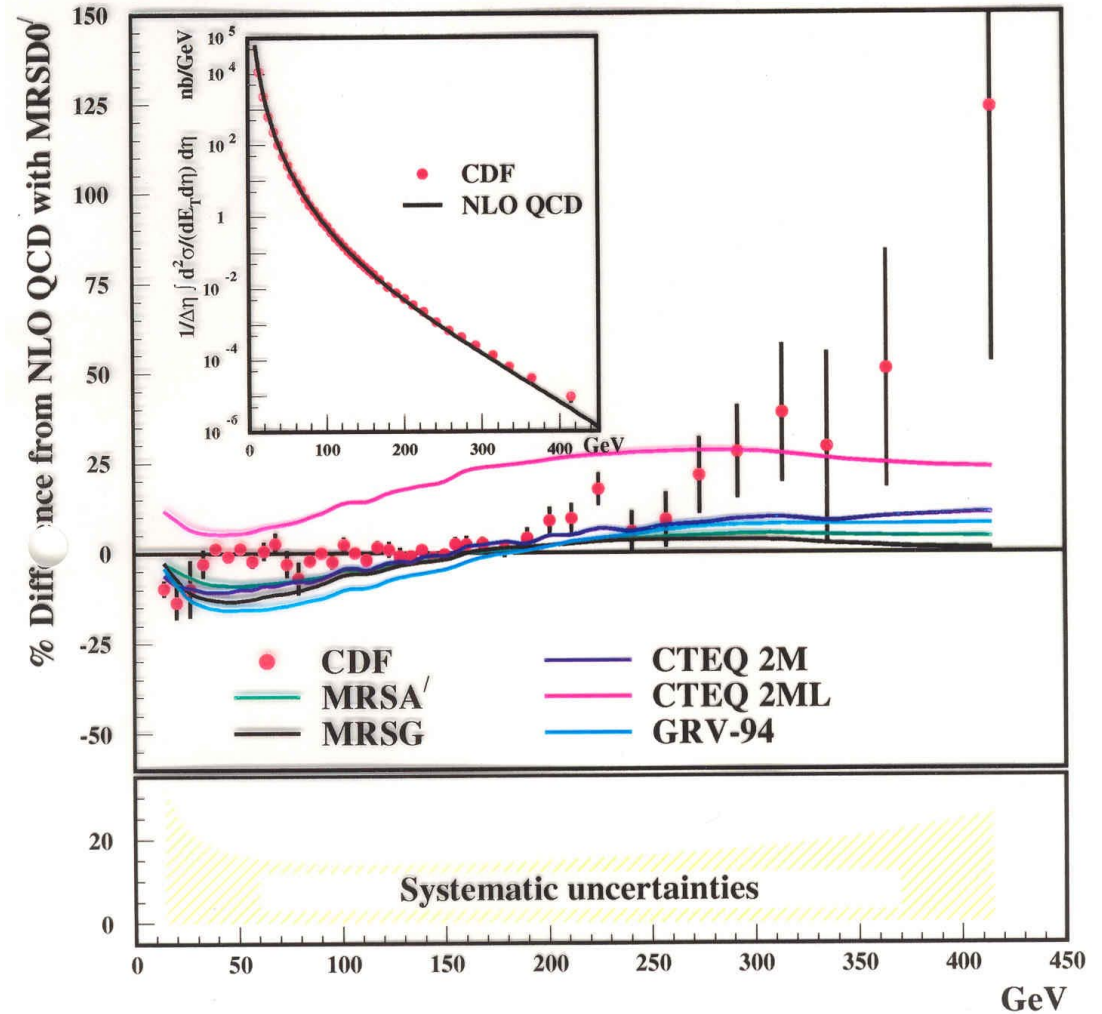


Figure 28: Inclusive jet cross section from the Run 1B data compared to a QCD prediction and to the published Run 1A data.

In the CDF 1995 inclusive jet data some excess was observed at $E_t > 200$ GeV over the current QCD predictions. In this plot the theory expectation was computed using the EKS (Ellis, Kunst and Stirling) structure functions.

None of the structure functions existing at that time set was able to predict the large E_t tail.



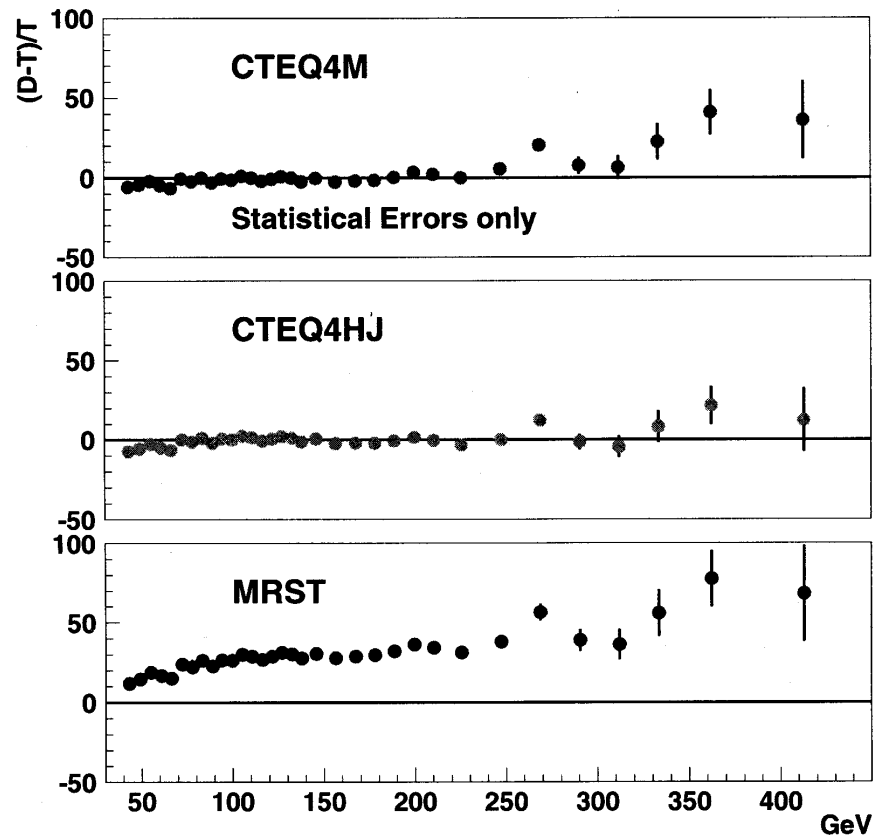


Figure 36: Run 1B data compared to QCD predictions (EKS, $\mu=E_T/2$, $R_{sep}=1.3$) using the CTEQ4M, CTEQ4HJ and MRST PDFs.

However, an updated set of structure functions, which used as input data also the Tevatron jet data (center plot), was able to make the anomaly disappear.

WHAT IF THE EXCESS RATE OF LARGE E_t JETS IS REAL?

If the excess cannot be reconciled with theory, the following possibilities exist:

- 1) The structure functions are inaccurate, as already mentioned
- 2) The jet energy scale of the experiment has a systematic error
- 3) The Monte Carlo evolving partons into jets is inaccurate
- 4) New physics.

The possibility of new physics in terms of parton substructures was considered and limits to the onset at large E_t of contributions by hard scattering between quark substructures were obtained. The best limits were obtained by comparing the angular distribution of dijet events to QCD expectations.

THE STUDY OF EXCLUSIVE DIJET CROSS SECTION

Exclusive dijet events can be selected with strict cuts limiting to 2 the number of energy clusters. Several studies can be made.

The dijet mass spectrum at large E_t can be searched for deviations indicative of quark sub-structures

The momenta of the scattered partons can be derived from the measured jet E_t and pseudorapidities, and their distribution can be readily compared with the effective proton structure function;

$$x_1 = \frac{E_t}{\sqrt{s}} \left(e^{\eta_1} + e^{\eta_2} \right), \quad x_2 = \frac{E_t}{\sqrt{s}} \left(e^{-\eta_1} + e^{-\eta_2} \right)$$

The dijet mass spectrum can be searched for bumps indicating new heavy particles decaying into 2 jets

After correcting for resolution smearing, the dijet cross section was still larger than QCD at masses ~ 400 GeV and higher.

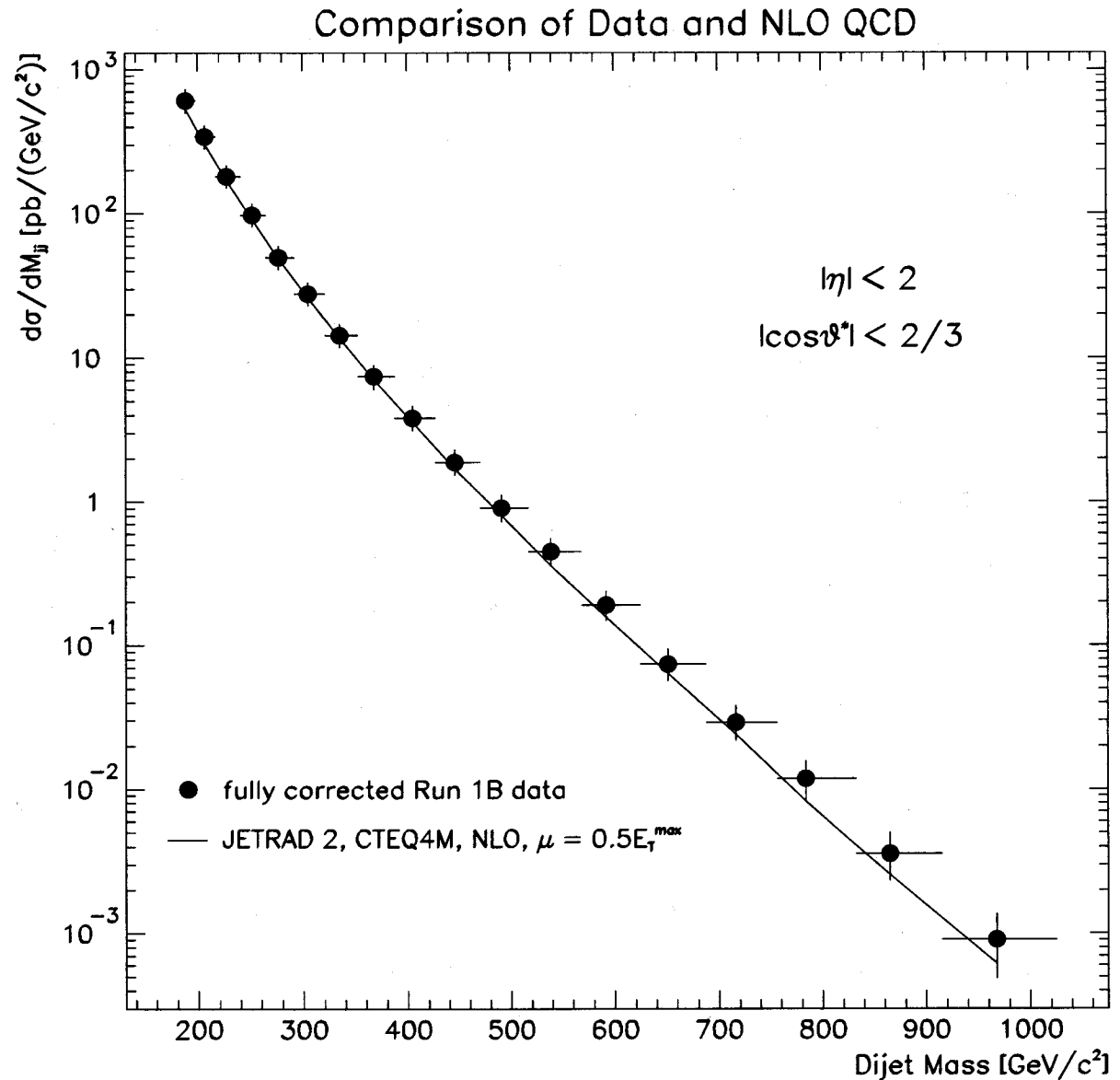
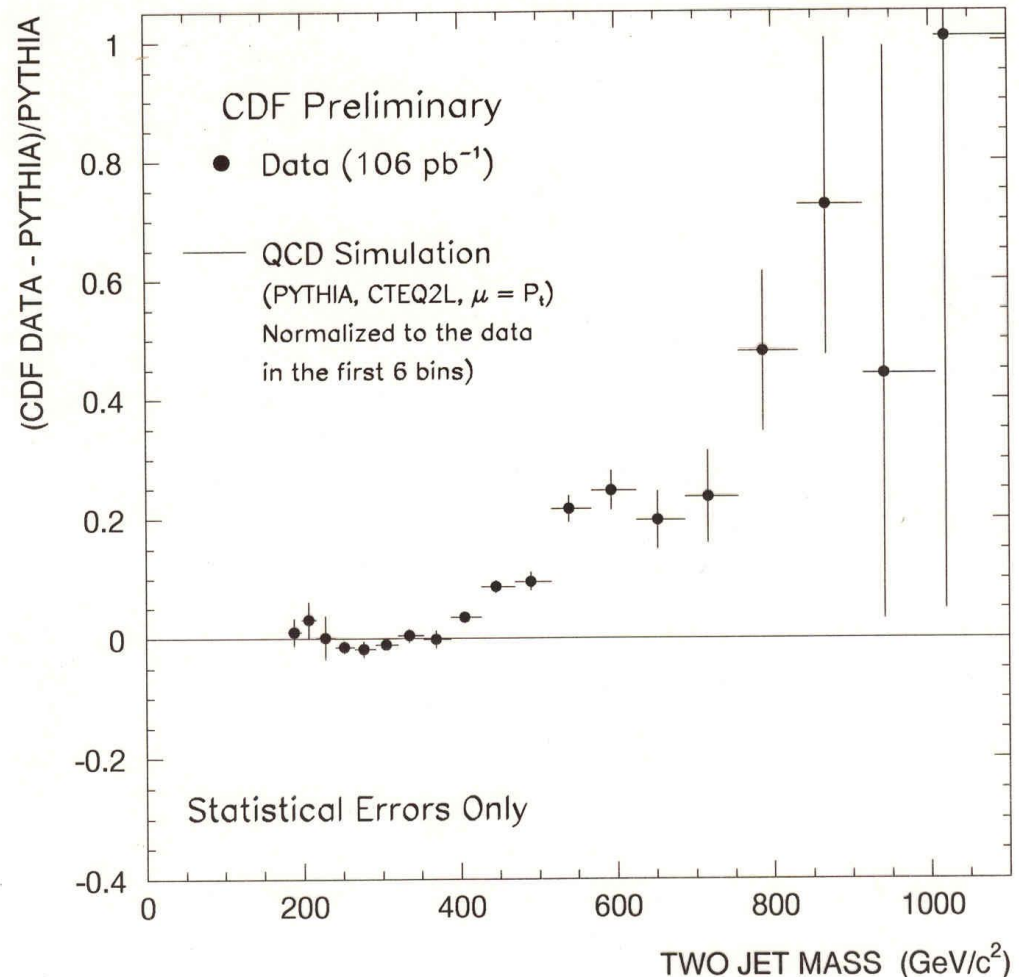


Figure 6.1: A comparison of the fully corrected data (full circles) with predictions from the JETRAD Monte Carlo program, using CTEQ4M and $\mu = 0.5E_T^{\max}$ (solid line). The bars represent the statistical and systematic uncertainties, added in quadrature.

Taken at face value the deviation of the CDF cross section from expectations at large masses looked significant. A critical study of the systematic uncertainties was made.

CDF Dijet Mass Distribution **Run 1A+1B**



A modified set of structure functions was developed by theorists that included the CDF data as input (CTEQ4M). The discrepancy with data was much reduced.

The large mass data were still above theory, but the deviations were within the systematic errors.

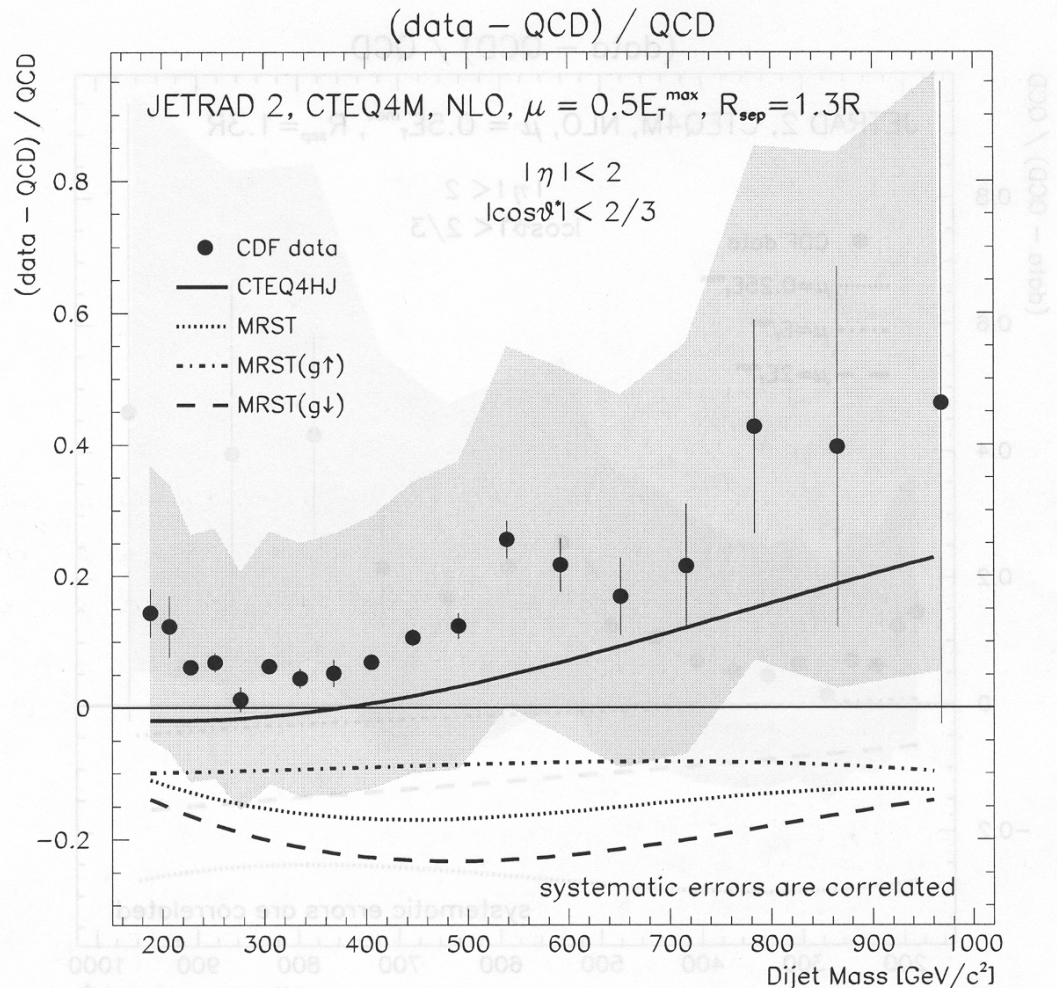


Figure 6.2: A comparison of our data with predictions from the JETRAD program for CTEQ4M (full circles) and comparisons of other parameterizations with CTEQ4M: CTEQ4HJ (solid), MRST (dotted), MRST($g \uparrow$)(dash-dotted) and MRST($g \downarrow$) (dashed). All QCD calculations were performed with $\mu = 0.5E_T^{max}$. The error bars indicate the statistical uncertainties and the shaded area represents the combined systematic uncertainty.

LIMIT TO QUARK SUBSTRUCTURES FROM DIJETS

If the deviation from QCD at large m_{jj} was real and due to a contribution from substructure scattering, the jet angular distribution would be sensitive to it.

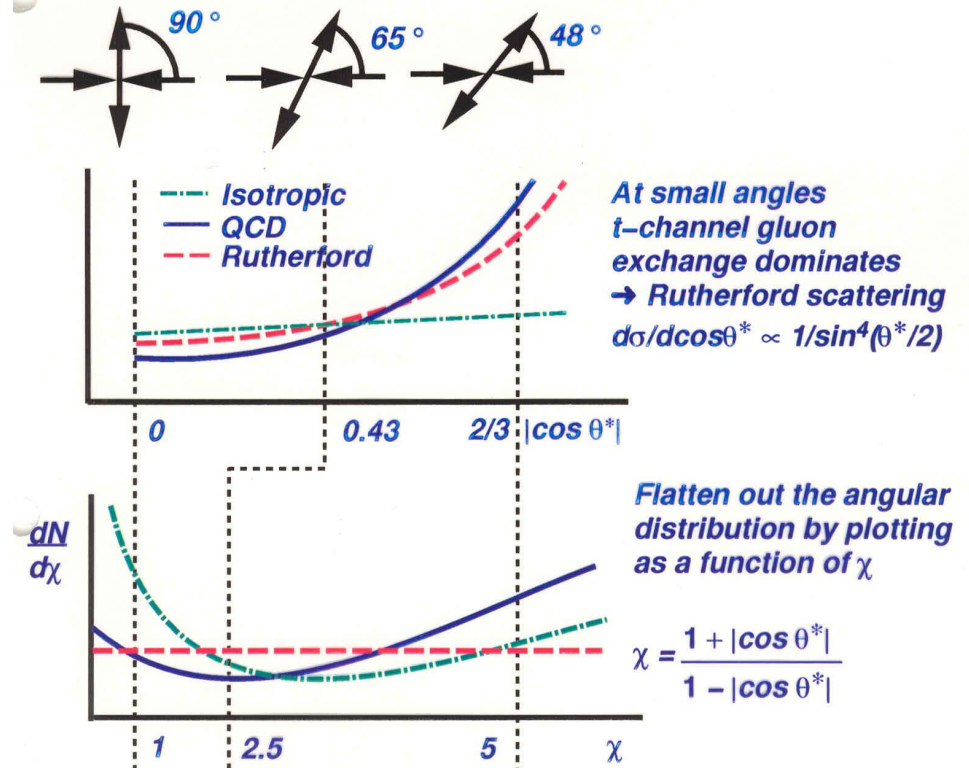
QCD amplitudes generate an approximate Rutherford scattering distribution. A point-like amplitude would generate a much flatter distribution.

The differences would be greatest at large $\cos\theta^*$. However, the detector is weakest in forward direction. It turned out to be best to study deviations as a function of a variable that emphasizes the differences at large polar angles.

$d\sigma/d\cos\theta^*$ is peaked forward and backwards in QCD as in Rutherford scattering, while the new term would be much flatter.

Since measurements around the beams are less precise, one chooses χ as a variable such that the difference would be large also at large angles.

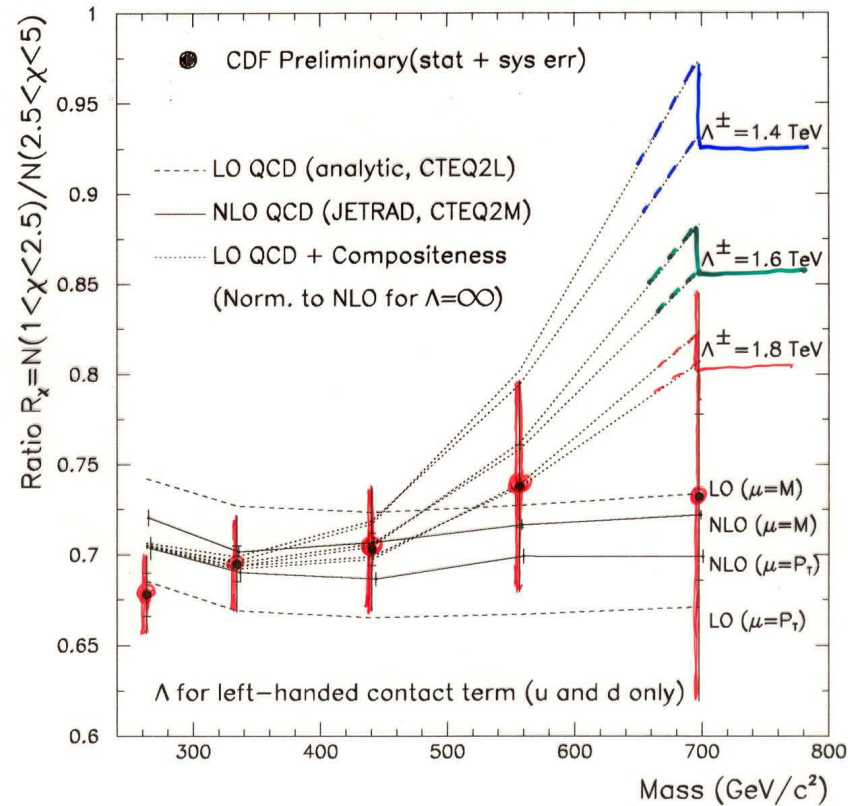
Dijet Angular Distribution



- $dN/d\chi$ is sensitive to new physics that has a more isotropic angular distribution than QCD (e.g. compositeness). For $\chi < 5$ the most sensitive variable is $R_\chi = N(\chi=1-2.5)/N(\chi=2.5-5)$
- Insensitive to PDF's
- Insensitive to overall energy scale but sensitive to η -dependence of calorimeter response and resolution

$$R_\chi = N(\chi = 1-2.5) / (N(\chi = 2.5-5))$$

Constraints on Compositeness from Dijet Angular Ratio



Systematic uncertainties : $\langle M_{jj} \rangle = 263 \text{ GeV} - 3\%$

$\langle M_{jj} \rangle = 698 \text{ GeV} - 14\%$

Compositeness limits : $\Lambda^+ \geq 1.6 \text{ TeV @ 95\% CL}$

$\Lambda^- \geq 1.4 \text{ TeV @ 95\% CL}$

THE MEASUREMENT OF THE W MASS AND WIDTH

When the weak interaction is mediated by the W,Z propagators, the intermediate boson masses are connected to the charged current Fermi coupling constant G_W , to the neutral current coupling constant G_Z and to the fine structure constant α

$$\frac{G_F}{\sqrt{2}} = \frac{e^2}{8M_W^2 \sin^2 \vartheta_W} = \frac{4\pi\alpha}{8M_W^2 \sin^2 \vartheta_W}$$

$$M_Z = \frac{M_W}{\cos \vartheta_W}$$

$$\frac{G_Z}{\sqrt{2}} = \frac{e^2}{8M_Z^2 \sin^2 \vartheta_W \cos^2 \vartheta_W} = \frac{e^2}{8M_W^2 \sin^2 \vartheta_W}$$

The ratio G_Z/G_F would be identically 1 in absence of “loop corrections” that are slightly different for M_W and M_Z :

$$\frac{G_Z}{G_W} = \frac{M_W^2}{M_Z^2 \cos^2 \vartheta_W} = \rho \approx 1$$

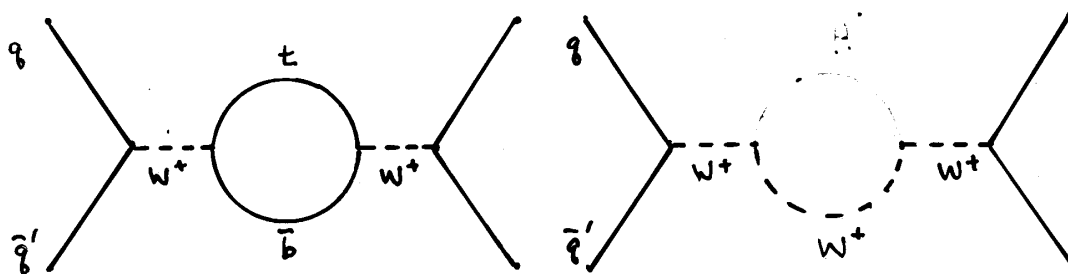
M_W is sensitive to squared fermion masses through loops like $W \rightarrow tb \rightarrow W$ and to log of the Higgs mass through $W \rightarrow HW \rightarrow W$ loops:

$$M_W = \sqrt{\frac{\pi\alpha}{\sqrt{2}G_F}} \frac{1}{\sin \vartheta_W} \frac{1}{\sqrt{1-\Delta R}}, \quad \Delta R = \text{loop correction} \propto \left(\frac{m_{top}}{M_W}\right)^2, \ln \frac{m_H}{M_W}$$

Radiative Corrections to the W Mass

$$\star M_W = \frac{A}{\sin \Theta_W \sqrt{1-\Delta R}} \text{ where } A = \left(\frac{\pi\alpha}{\sqrt{2}G_F}\right)^{\frac{1}{2}}$$

$$\star \Delta R \sim \left(\frac{M_{Top}}{M_W}\right)^2, \ln \frac{M_H}{M_W}$$



Within the Standard Model an accurate measurement of M_W provides a measurement of the sum of the contributions of the top and of the Higgs loops, and allows to constrain their masses.

THE MEASUREMENT OF THE W MASS

The request of an isolated large E_t electron or muon is already enough to isolate a sample of events rich in $W \rightarrow e\nu$, $W \rightarrow \mu\nu$.

About 20% of the W events have one or more jets recoiling against the W . The W transverse mass distribution is slightly affected by the W transverse momentum.

For a precise measurement of the W mass through the observed transverse mass distribution, gluon radiation must be well modeled in order to input in the simulation the correct W p_t distribution and be able to predict the transverse mass as a function of the parameters to be measured, M_W and Γ_W .

The request of an isolated good quality electron is sufficient in CDF to get a clear jacobian peak both in the electron E_t and in the $E_{t,miss}$ distribution.

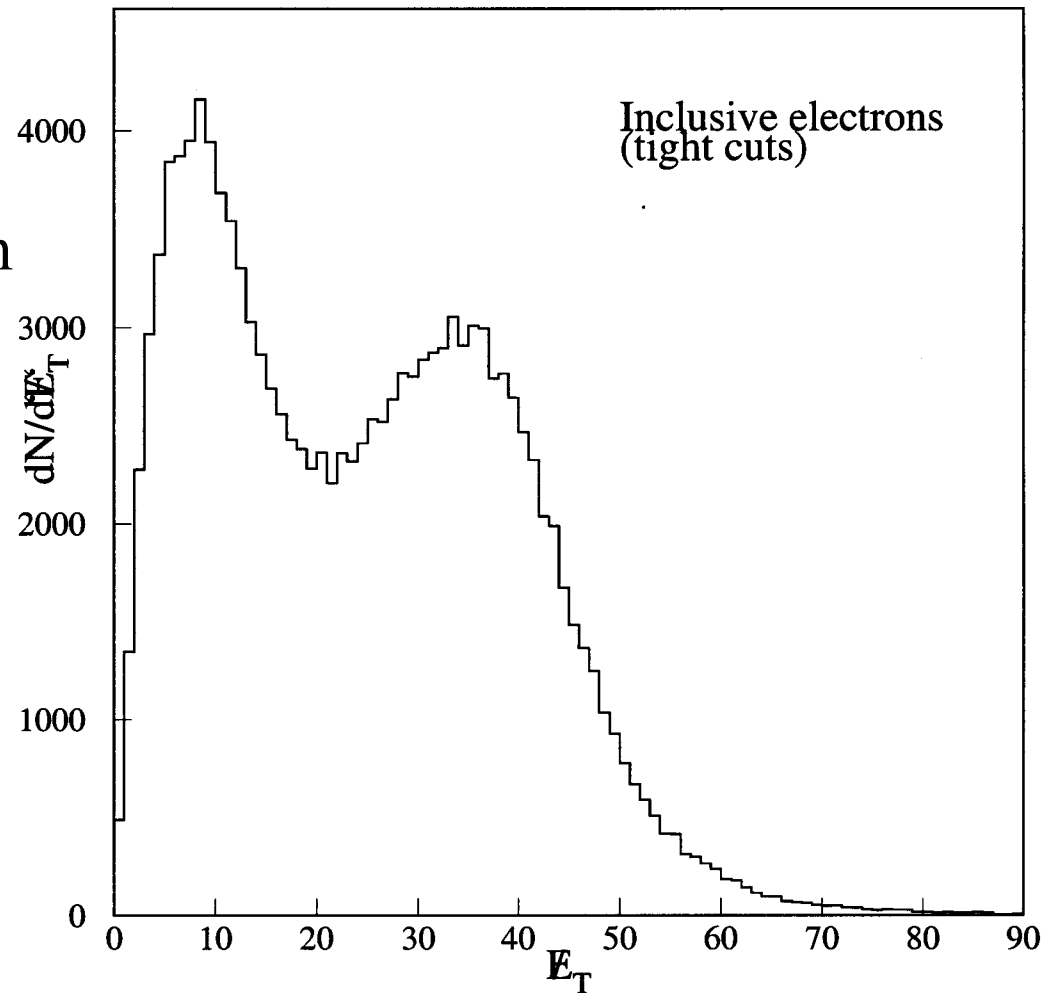


Figure 3.3: The plot shows the E_t distribution for the inclusive electron sample. Noticeable is the W peak due to the escaped ν .

MEASURING AN ABSOLUTE NUMBER LIKE M_W

Measuring an absolute number is always a delicate problem.

The M_W measurement in the muon channel depends on the CTC momentum scale being correct.

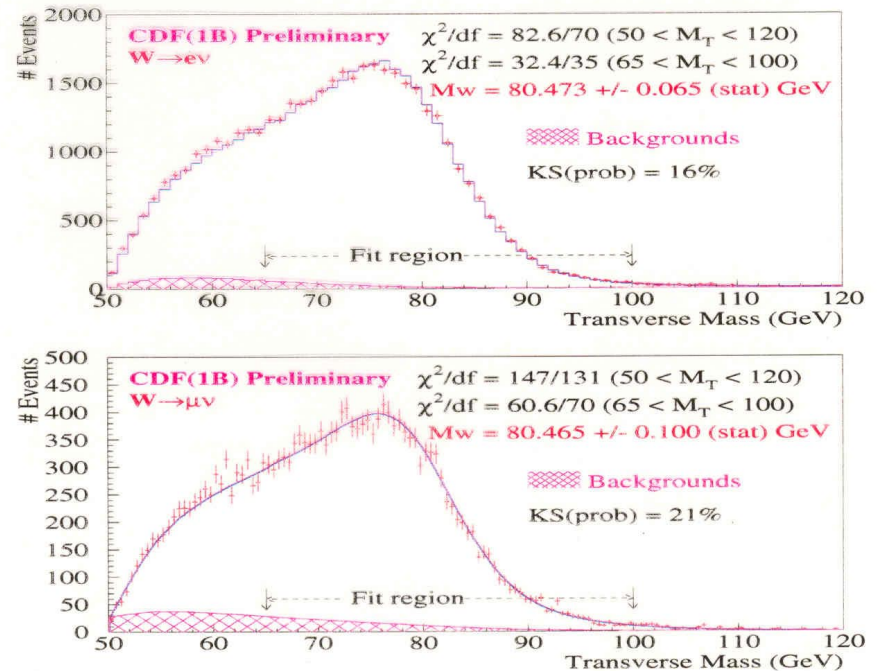
The magnetic field is mapped accurately and the resulting bending power is checked against the reconstructed j/ψ , Y , Z masses which are precisely known.

The e.m. calorimeter energy scale obtained with calibrations on test beams has a very large error compared to the goal of the M_W measurement ($\sim 1/2$ per thousand). This accuracy can be reached by transferring the momentum calibration of the CTC to the e.m. calorimeter energy calibration using isolated electrons. However this is a delicate task because electrons radiate while passing through the chamber.

The W mass is derived from a fit to the m_T in both the electron and the muon channel by CDF.

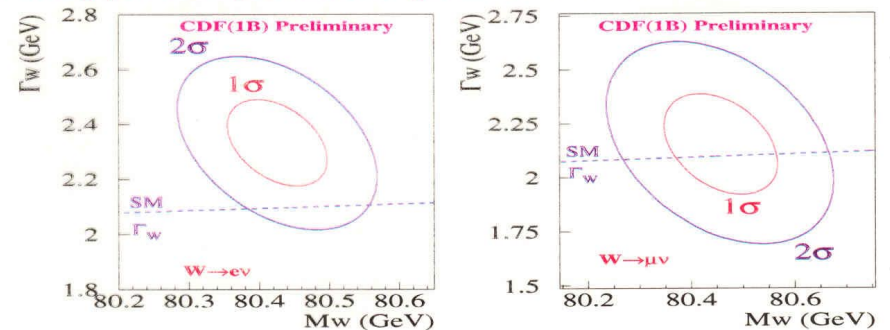
The width Γ_W can either be input to its S.M. value or left free in the fit.

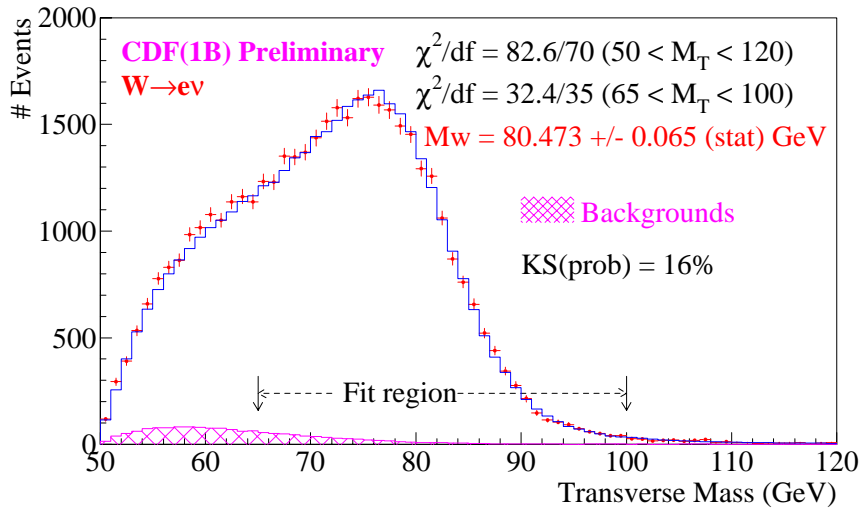
Transverse Mass Fits



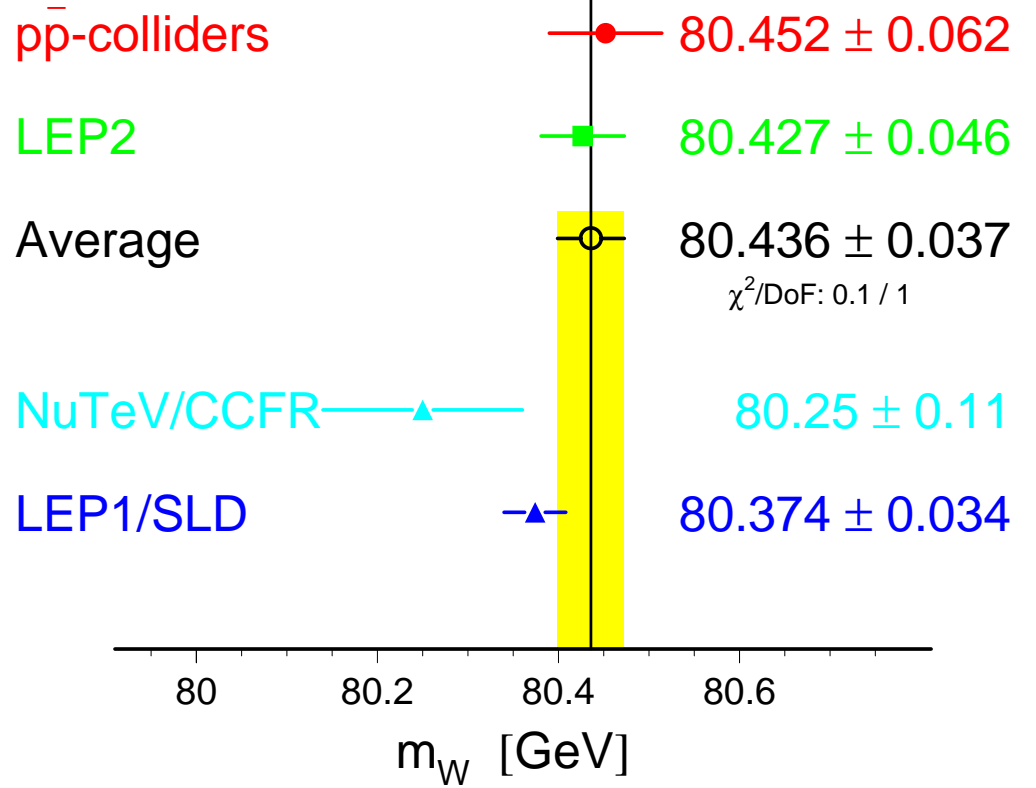
The above fits have Γ_W fixed to SM predictions.

Fitting for both parameters yields consistent results:





W-Boson Mass [GeV]



DRELL-YAN ABOVE THE Z

The Z contribution is derived by fitting the peak over the smoothly decreasing D.Y. cross section.

Deviations from D.Y. at large pair mass may indicate the existence of more massive Z's, or of internal quark/lepton structures.

$$\sigma_{\gamma,Z} Br(\gamma, Z \rightarrow ee, \mu\mu) \text{ (Run Ia + Ib)}$$

